J|A|C|S
ARTICLES
Published on Web 11/16/2007

The Many Ways To Have a Quintuple Bond

Gabriel Merino,*[,‡] Kelling J. Donald,[†,§] Jason S. D'Acchioli,[#] and Roald Hoffmann*[,§]

Contribution from the Facultad de Química, Universidad de Guanajuato, Noria Alta s/n CP 36050, Guanajuato, Gto. México, Department of Chemistry & Chemical Biology, Cornell University, Ithaca, New York 14853, and Department of Chemistry, University of Wisconsin—Stevens Point, Stevens Point, Wisconsin 54481

Received July 21, 2007; E-mail: gmerino@quijote.ugto.mx, rh34@cornell.edu

Abstract: The existence and persistence of five-fold (quintuple) bonding in isomers of model RMMR molecules of quite different geometry are examined theoretically. The molecules studied are RMMR, with R = H, F, Cl, Br, CN, and CH_3; M = Cr, Mo, and W. The potential energy surface of these molecules is quite complex, containing two, three, even four local minima. The structural preferences in these molecules are rationalized, and electronic factors responsible for these preferences are elucidated. The linear geometry is always a minimum, but almost never the global minimum; there is a definite preference in RMMR for either a *trans*-bent conformation or perturbations of the *trans*-bent isomer with at least one of the R groups in a bridging position about the MM bond. The potential energy surface of these RMMR molecules is relatively flat, the lowest energy conformation being that which for a given molecule attains the best compromise between maximization of the MM bonding and minimization of orbital interactions that are MR antibonding. A surprising low-symmetry C_s structure is identified, which along with the *trans*-bent isomer is one of the two most popular choices for the global minimum. Regardless of what isomer of the RMMR molecule is preferred, the MM quintuple bond persists.

Introduction

Until the mid 1960s, it was generally believed that the highest bond order attainable between any two elements of the periodic table was three. The existence of the first quadruple metal−metal bond (in the $Re_2Cl_8^{2-}$ anion) was recognized by Cotton and Harris in 1965.[1,2] Since then, hundreds of other compounds with formally quadruply bonded transition metal atoms have been synthesized, and the characteristics (length, energetics, spectroscopic signatures) of metal−metal quadruple bonding have been explored in detail.[3]

The quest for complexes with even higher bond orders has continued. If we think of a bond as a variable-strength coupling of two electrons then, in principle, pairs of electrons can form up to nine bonds using all the valence s, p, and d orbitals of two transition metal centers.[4] So, it should be possible to move beyond quadruple bonding. In fact, there has been a lively discussion in the literature — both experimental[5−13] and theo-

‡ Universidad de Guanajuato.
§ Cornell University.
# University of Wisconsin−Stevens Point.
† Current address: Department of Chemistry, Gottwald Center for the Sciences, University of Richmond, Richmond, VA 23173.

(1) Cotton, F. A.; Harris, C. B. *Inorg. Chem.* **1965**, *4*, 330.
(2) Cotton, F. A.; Curtis, N. F.; Johnson, B. F. G.; Mague, J. T.; Wood, J. S.; Harris, C. B.; Robinson, W. R.; Lippard, S. J. *Science* **1964**, *145*, 1305.
(3) Cotton, F. A.; Murillo, C. A.; Walton, R. A. *Multiple bonds between metal atoms*, 3rd ed.; Springer Science and Business Media Inc.: New York, 2005.
(4) For an important discussion of multiple bonding across the periodic table, see: Roos, B. O.; Borin, A. C.; Gagliardi, L. *Angew. Chem., Int. Ed.* **2007**, *46*, 1469.
(5) Kundig, E. P.; Moskovits, M.; Ozin, G. A. *Nature* **1975**, *254*, 503.
(6) Klotzbucher, W.; Ozin, G. A. *Inorg. Chem.* **1977**, *16*, 984.
(7) Gupta, S. K.; Atkins, R. M.; Gingerich, K. A. *Inorg. Chem.* **1978**, *17*, 3211.
(8) Weltner, Jr. W.; Van Zee, R. J. *Annu. Rev. Phys. Chem.* **1984**, *35*, 291 and references therein.
(9) Morse, M. D. *Chem. Rev.* **1986**, *86*, 1049.
(10) Xiao, Z. L.; Hauge, R. H.; Margrave, J. L. *J. Phys. Chem.* **1992**, *96*, 636.
(11) (a) Casey, S. M.; Villalta, P. W.; Bengali, A. A.; Cheng, C. L.; Dick, J. P.; Fenn, P. T.; Leopold, D. G. *J. Am. Chem. Soc.* **1991**, *113*, 6688. (b) Casey, S. M.; Leopold, D. G. *J. Phys. Chem.* **1993**, *97*, 816. (c) Casey, S. M.; Leopold, D. G. *Chem. Phys. Lett.* **1993**, *201*, 205.
(12) Chisholm, M. H.; Macintosh, A. M. *Chem. Rev.* **2005**, *105*, 2949.
(13) Nguyen, T.; Sutton, A. D.; Brynda, S.; Fettinger, J. C.; Long, G. J.; Power, P. P. *Science* **2005**, *310*, 844.
(14) (a) Kant, A.; Strauss, B. *J. Phys. Chem.* **1966**, *45*, 3161. (b) Norman, J. G.; Kolari, H. J.; Gray, H. B.; Trogler, W. C. *Inorg. Chem.* **1977**, *16*, 987. (c) Atha, P. M.; Hillier, I. H.; Guest, M. F. *Chem. Phys. Lett.* **1980**, *75*, 84. (d) Bursten, B. E.; Cotton, F. A.; Hall, M. B. *J. Am. Chem. Soc.* **1980**, *102*, 6348. (e) Kok, R. A.; Hall, M. B. *J. Phys. Chem.* **1983**, *87*, 715. (f) Hall, M. B. *Polyhedron* **1987**, *6*, 679.
(15) (a) Goodgame, M. M.; Goddard, W. A. *J. Phys. Chem.* **1981**, *85*, 215. (b) Goodgame, M. M.; Goddard, W. A. *Phys. Rev. Lett.* **1982**, *48*, 135. (c) Goodgame, M. M.; Goddard, W. A. *Phys. Rev. Lett.* **1985**, *54*, 661.
(16) Udovic, B. *Proc. Indian Acad. Sci.−Chem. Sci.* **1998**, *110*, 471.
(17) Yanagisawa, S.; Tsuneda, T.; Hirao, K. *J. Chem. Phys.* **2000**, *112*, 545.
(18) Barden, C. J.; Rienstra-Kiracofe, J. C.; Schaefer, H. F. *J. Chem. Phys.* **2000**, *113*, 690.
(19) (a) Boudreaux, E. A.; Baxter, E. *Int. J. Quantum Chem.* **2001**, *85*, 509. (b) Boudreaux, E. A.; Baxter, E. *Int. J. Quantum Chem.* **2004**, *100*, 1170. Erratum: *Int. J. Quantum Chem.* **2005**, *105*, 199.
(20) Kraus, D.; Lorenz, Bondybey, M. V. E. *Phys. Chem. Comm.* **2001**, *4*, 44.
(21) Gutsev, G. L.; Bauschlicher, C. W. *J. Phys. Chem. A* **2003**, *107*, 4755.
(22) Jules, J. L.; Lombardi, J. R. *J. Phys. Chem. A* **2003**, *107*, 1268.
(23) (a) Roos, B. O. *Collect. Czech. Chem. Commun.* **2003**, *68*, 265. (b) Roos, B. O.; Malmqvist, P. A.; Gagliardi, L. *J. Am. Chem. Soc.* **2006**, *128*, 17000. (c) Roos, B. O.; Borin, A. C.; Gagliardi, L. *Angew. Chem., Int. Ed.* **2007**, *46*, 1469.
(24) (a) Frenking, G. *Science* **2005**, *310*, 796. (b) Frenking, G.; Tonner, R. *Nature* **2007**, *446*, 276.
(25) Schultz, N. E.; Zhao, Y.; Truhlar, D. G. *J. Phys. Chem. A* **2005**, *109*, 4388.
(26) Gagliardi, L.; Roos, B. O. *Nature* **2005**, *433*, 848.
(27) Weinhold, F.; Landis, C. R. *Valency and Bonding: A Natural Bond Orbital Donor-Acceptor Perspective*; Cambridge University Press: Cambridge, UK/New York, 2005; p ix.
(28) Landis, C. R.; Weinhold, F. *J. Am. Chem. Soc.* **2006**, *128*, 7335.
(29) Brynda, M.; Gagliardi, L.; Widmark, P. O.; Power, P. P.; Roos, B. O. *Angew. Chem., Int. Ed.* **2006**, *45*, 3804.

retical[8,9,12−31] — of quintuple and sextuple bonding. For example, there is now ample experimental evidence, mainly from matrix isolation IR and UV−vis spectroscopic studies over the past 40 years, for the existence of the formally sextuply bonded Cr_2 and Mo_2[5−12,14a] molecules (less so for W_2[20]). To be sure, the details of the bonding in these diatomic species are still not completely resolved. Yet, there is a general consensus that both Cr_2 and Mo_2 are singlets ($^1\Sigma^+$) in their ground states (see, e.g., refs 8, 19b, 20, 21, and 32) and have a very short interatomic separation, suggesting that the six *n*s and $(n-1)$d valence electrons from each metal atom are paired up in some way.[33,34]

Recently, Nguyen et al. published the first evidence for a molecule with a kinetically persistent quintuple bond.[13] In that work, they argued convincingly from experimental and computational analyses that in the dichromium complex Ar′CrCrAr′ (where Ar′ is the bulky C_6H_3-2,6(C_6H_3-2,6-^{i}Pr$_2$)$_2$ ligand; ^{i}Pr = isopropyl fragment) the two chromium atoms share five electron pairs in five bonding molecular orbitals.

Along with the unusually large presumed bond order in Ar′CrCrAr′, the complex is of interest from a structural point of view. The bulky Ar′ groups are *trans* to each other, such that the local symmetry about the Cr_2 fragment is C_{2h}, not linear. And there are certainly signs of interaction between the Ar′ ring and the distal Cr.[13]

In the present work, we try to rationalize the structural preferences in quintuply bonded systems and the electronic factors behind them. The computational details are given in the Appendix to this paper (see the Supporting Information). We investigate the structural preference in a series of simple RMMR complexes (R = H, F, Cl, Br, CN, and the methyl group (CH_3), abbreviated Me; M = Cr, Mo, and W). The R groups were chosen to cover a range of donor and acceptor character. In this exercise we got a number of surprises. And we think we have gained much of the chemical insight needed for a discussion of model complexes with bulkier substituents, which we will describe in a separate contribution.

Bonding in Group 6 M_2 Dimers

On the way to the more complicated RMMR structures we begin with a theoretical analysis of the M_2 (M = Cr, Mo, W) fragment. The one-electron interaction diagram for Mo_2 is shown in Figure 1.

The sextuple bonding configuration for the M_2 (Cr_2, Mo_2, W_2) fragment corresponds to filling two σ-type orbitals (formally, one from the d block and one from the s orbitals), plus two π-type and two δ-type orbitals. In reality, of course, there is substantial configuration mixing, which has been extensively studied for these dimers (see ref 23a).

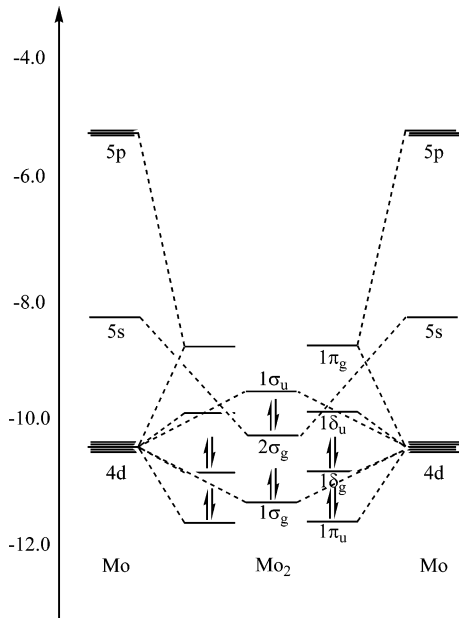

Figure 1. Orbital interaction diagram showing the valence energy levels for Mo and Mo_2. The energy levels come from an extended Hückel calculation.

In this paper, the M_2 units, as interesting as they are, are not themselves our focus. The diatomics serve us as building blocks for the neutral RMMR molecules (R = one-electron σ donors: H, F, Cl, Br, CN, and Me, all viewed as neutral ligands). The orbitals of the linear RMMR are not difficult to construct. The R groups deliver two hybrids (or s or p orbitals, as the case may be) which transform as σ_g and σ_u, and these interact with the M_2 orbitals, primarily $2\sigma_g$ and $1\sigma_u$ of Figure 1. The resulting MH bonding combinations (σ_g and σ_u) take four electrons — two formally from M and two from the ligands. The remaining five mainly M−M bonding orbitals (one σ_g, two π_u, and two δ_g) are occupied by 10 electrons. That is the formal quintuple bond of the Nguyen et al. compound.[13] We will see these orbitals explicitly later on in our paper.

One lesson of the experimentally observed compound reported by Nguyen et al.[13] (and from what we know of multiply bonded group 14 compounds[35]) is that it is not advisable to restrict oneself to a linear conformation; one must proceed to look to a wider range of geometries. This we do now.

Structural Preferences in Simple RMMR Complexes

We began an exploration of the potential energy surface (PES) of RMMR molecules (M = Cr, Mo, W; R = H, F, Cl, Br, CN, and Me). The halide and cyanide substituents were chosen as models of π-donors and acceptors, respectively (the hydrides have been considered previously by Landis and Weinhold[27,28]). For the five molecules, geometrical optimizations were performed for six starting geometries, namely the C_{2h} *trans*-bent (**1**), linear (**2**), *cis*-bent (**3**), D_{2h} doubly bridged (**4**), C_{2v} doubly bridged (**5**), and the lower symmetry singly bridged C_s (**6**) isomers (see Figure 2). The computed geometric parameters are listed in Table 1. For each molecule, the geometries and relative energies, ΔE, for the lowest energy isomer are in bold type (Table 1). The number of imaginary frequencies obtained for each of the optimized structures is given in the Supporting Information, Table 1-SI.

(30) Weinhold, F.; Landis, C. R. *Science* **2007**, *316*, 61.
(31) Wu, X.; Lu, X. *J. Am. Chem. Soc.* **2007**, *129*, 2171.
(32) Celani, P.; Stoll H.; Werner H.-J.; Knowles P. J. *Mol. Phys.* **2004**, *102*, 2369.
(33) In the case of Cr_2, there is a diversity of perspectives on the bonding (that's a gentle way of describing the disagreement). Our opinion, on reviewing the literature, is the theoretical calculations suggest a five-fold covalent bond involving the 10 d electrons, the s electrons being antiferromagnetically coupled and localized each primarily on one of the Cr atoms. A similar bonding pattern (a combination of covalent bonds and antiferromagnetically coupled electron pairs) has been suggested for Mo_2, as well. The suggestion that the s electrons are nonbonding in Cr_2 is consistent with an observed insensitivity of the Cr−Cr bond to the $^1\Sigma_g^+ \rightarrow {}^3\Sigma_u^+$ excitation (see ref 15).
(34) For the actinides, there are still more orbitals available for bonding. In a recent study, illustrative of the complexities of the field (ref 26), Gagliardi and Roos suggested that the U_2 molecule is quintuply bonded but, rather than simply so, in a complex bonding pattern in which 10 electrons reside in 16 U_2 molecular orbitals that are very close in energy.
(35) Sekiguchi, A.; Kinjo, R.; Ichinohe, M. *Science* **2004**, *305*, 1755.

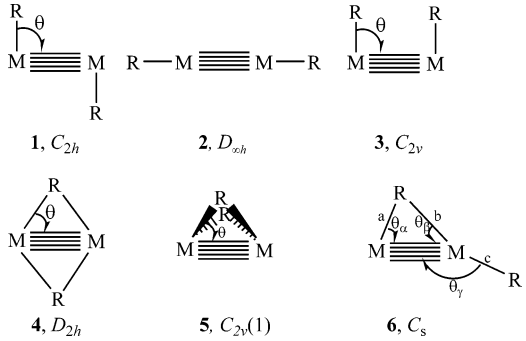

Figure 2. Possible isomers of the RMMR molecules (R = H, F, Cl, Br, CN, and Me; M = Cr, Mo, and W).

The reader may wonder why we picked these geometries. The observed C_{2h} and the simplistically postulated $D_{\infty h}$ are obvious choices. Usually, where there is *trans*-bending, one should look for a *cis*-bent geometry (e.g., excited states of acetylene). The D_{2h} structure is a "symmetrization" of the *trans*-bent geometry; $C_{2v}(1)$, a puckered variant, is known for Si_2H_2. And the C_s structure, to put it frankly, just turned up in optimizations.

For R = Me, the geometries have to be defined more carefully, given rotational possibilities for the methyl group. The geometries that eventually survive as minima are shown in Figure 3.

The linear ($D_{\infty h}$) structure is a local minimum for all 15 of the RMMR molecules studied; a detailed vibrational analysis finds no imaginary vibrational frequency for that geometry. However, the linear structure is the lowest energy isomer in only two cases, namely FCrCrF and ClCrCrCl. In fact, although the linear isomer is competitive for many of the other chromium and molybdenum complexes, it is one of the highest energy structures for the tungsten systems.

The *cis*-bent C_{2v} structure is a local minimum on the PES for all the hydrides and the fluorides but is always less stable (by 6−18 kcal·mol^{-1}) than the *trans*-bent C_{2h} form. For the larger halides (R = Cl and Br), the *cis*-bent isomer typically collapses to the linear geometry. In all cases except for R = CN, the intriguing $C_{2v}(1)$ structures optimizes to the D_{2h} isomer.

Apart from the two cases mentioned previously for which the linear isomer is preferred, the lowest energy isomers are either the C_{2h}, D_{2h}, or C_s structures. The symmetrically doubly bridging D_{2h} structure (the computed global minimum for BrCrCrBr only) is a surprise, as is the singly bridging C_s structure (the global minimum for a number of structures). A typical C_s structure, for FMoMoF, is shown in Figure 4.

Are the Various Minima Real?

The question has two sides to it: (1) Are the geometries an artifact of the computational methodology, and (2) are some of the minima so shallow as to be physically unimportant?

We will face up to the second question in a while. On the first one, the geometrical conclusions of Table 1 are for a specific software package, functional, and basis set. We are painfully aware, from experience with other molecules, that there is no good error analysis in this business, and that stability

Table 1. Computed Geometrical Parameters of the Local Minima on the PES of RMMR (R = H, F, Cl, Br, CN, and Me), at the BLYP Level[a,b] (bond lengths are given in picometers, angles in degrees, and $\Delta E_{rel} = \Delta E$(isomer) − $\Delta E(D_{\infty h})$ in kcal·mol^{-1})

		Cr				Mo				W			
		M–M	M–R	θ	ΔE_{rel}	M–M	M–R	θ	ΔE_{rel}	M–M	M–R	θ	ΔE_{rel}
H	C_{2h}	**171**	**164**	**89**	**−9**	**208**	**173**	**91**	**−19**	**212**	**171**	**93**	**−32**
	$D_{\infty h}$	165	167	180	[0]	202	179	180	[0]	204	174	180	[0]
	C_{2v}	173	162	109	9	210	171	99	−9	214	170	97	−26
F	C_{2h}	*Not a Minimum*				211	198	103	−2	**217**	**192**	**108**	**−36**
	$D_{\infty h}$	**164**	**181**	**180**	**[0]**	200	198	180	[0]	203	191	180	[0]
	C_{2v}	178	180	110	20	212	195	106	7	217	192	105	−29
	C_s	174	*	*	3	**209**	*	*	**−4**	*Optimizes to C_{2h} Structure*			
Cl	C_{2h}	*Optimizes to D_{2h} Structure*				*Not a Minimum*				**215**	**234**	**106**	**−32**
	$D_{\infty h}$	**164**	**210**	**180**	**[0]**	201	237	180	[0]	202	232	180	[0]
	C_{2v}	*Optimizes to $D_{\infty h}$ Structure*				*Optimizes to $D_{\infty h}$ Structure*				216	233	108	−24
	D_{2h}	169	247	70	3	*Not a Minimum*				*Not a Minimum*			
	C_s	172	*	*	2	**208**	*	*	**−5**	*Optimizes to C_{2h} Structure*			
Br	C_{2h}	*Optimizes to D_{2h} Structure*				*Not a Minimum*				**215**	**248**	**104**	**−31**
	D_h	164	234	180	[0]	201	237	180	[0]	202	246	180	[0]
	C_{2v}	*Optimizes to $D_{\infty h}$ Structure*				*Optimizes to $D_{\infty h}$ Structure*				216	247	109	−22
	D_{2h}	**169**	**259**	**71**	**−3**	*Not a Minimum*				*Not a Minimum*			
	C_s	*Optimizes to D_{2h} Structure*				**208**	*	*	**−6**	214	*	*	−30
CN	C_{2h}[c]	**174**	**210**	**67**	**−22**	*Not a Minimum*				*Not a Minimum*			
	$D_{\infty h}$	164	202	180	[0]	201	217	180	[0]	203	208	180	[0]
	C_{2v}	*Optimizes to $D_{\infty h}$ Structure*				211	210	106	−5	217	204	103	−35
	C_s	*Optimizes to C_{2h} Structure*				**210**	*	*	**−24**	**215**	*	*	**−50**
Me	C_{2h}	*Not a Minimum*				**209**	**218**	**98**	**−11**	**214**	**214**	**102**	**−23**
	D_{3d}	166	206	180	[0]	203	220	180	[0]	206	216	180	[0]
	C_{2v}	*Optimizes to D_{3d} Structure*				*Not a Minimum*				215	213	108	−18
	C_s	**172**	*	*	**−2**	*Optimizes to C_{2h} Structure*				*Optimizes to C_{2h} Structure*			

[a] See Figure 2 for the structures to which the symmetry labels refer. [b] A more complete table in the Supporting Information gives the transition structure geometries (Table 2-SI). The number of imaginary frequencies obtained for each of the optimized structures is given in the Supporting Information (Table 1-SI). [c] For R = H, F, Cl, and Br the $C_{2v}(1)$ structure collapses to a near D_{2h} structure. For $Cr_2(CN)_2$ and $Mo_2(CN)_2$, the $C_{2v}(1)$ structure converges to saddle points in which the dihedral angles between the two MCM planes are 119.8° and 120.7°, respectively. See Figure 3-SI for an example of the geometries obtained for the cyano complexes. *Details of the geometry of the C_s structures are given in Table 2-SI in the Supporting Information. Boldface marks the lowest energy structure for each entry.

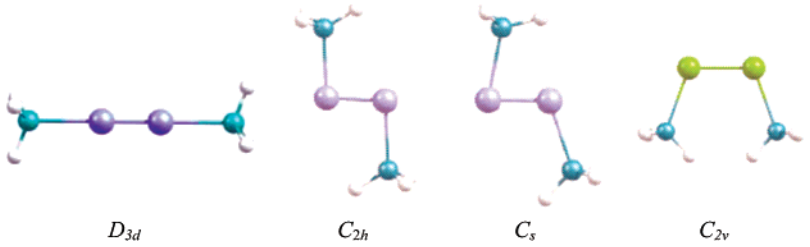

Figure 3. Geometries of the MeMMMe structures that are local minima, at the BLYP level, for at least one of the compounds we consider. All the structures, including less competitive ones than these, are shown in Figure 1-SI of the Supporting Information.

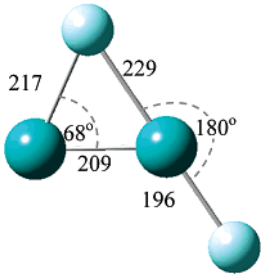

Figure 4. Minimum energy (C_s) geometry of FMoMoF. The bond distances are in picometer units.

conclusions may vary with method. So we repeated some of the calculations with the following methods; the results are given in the Supporting Information.

Our calculations for the HCrCrH isomers have been repeated using different functionals: the B3LYP variant of Becke's three-parameter hybrid functional, combined with the correlation function of Lee, Yang, and Parr, and the so-called PW91 method employing the exchange and correlation functionals of Perdew and Wang (see Table 3-SI). The 6-31G* basis set was used on H, and the SDD basis set and ECP were used at the Cr centers (the calculations were repeated using the LANL2DZ basis set and ECP at the Cr centers).

In another series of studies, we examined the RCrCrR hydride and halide compounds listed in Table 1 (R = H, F, Cl, and Br) using a variety of available density functional methods and basis sets: the BLYP, BP86, PBE, and the OLYP DFT methods in combination with the double-ζ polarized (DZP) (and separately the triple-ζ polarized, TZ2P) basis set on all atomic sites. The range of (single configurational) methods admittedly does not include a state-of-the-art treatment of correlation. We have, nonetheless, been encouraged by the fact (see Supporting Information, Tables 4-SI and 5-SI) that the structural trends summarized in Table 1 survive pretty well through the spread of model chemistries examined.

Our general conclusion, derived from these calculations, is that the occurrence of the various minima — linear, *trans*- and *cis*-bent, and C_s — persists, with generally small but sometimes significant variation in relative energies and bond distances (as much as 10 pm differences in the distances, depending on the method).

To respond intelligently to the second question concerning the depth of the minima, we need to have an idea of the general shape of the potential energy surfaces for RMMR. Computational searches for transition states for the interconversion of the various minima were found to be time-consuming and were in general non-convergent. We got a good feeling for the surfaces from constrained transits across the surface. For instance, Figure 5 shows a transit for HCrCrH from the *cis*-bent C_{2v} minimum to the linear geometry, and from the linear geometry to the *trans*-bent C_{2h} minimum. In each case, the angle θ was used as a reaction coordinate, changed incrementally, and all the remaining geometrical parameters were optimized within that symmetry constraint.

The essential features are (a) a significant barrier (>10 kcal·mol^{-1}) between the *trans* and linear isomers (Brynda et al. obtained 20 kcal·mol^{-1} for the similar barrier in the phenyl analogue, PhCrCrPh),[29] (b) a very small barrier between the *cis* and linear ones, and (c) energetic curves steeply rising with θ on the *cis* side. We also tested a direct *cis*-to-*trans* transit by a rotation around the CrCr bond, through a hydrogen peroxide-type waypoint. This faced a substantially higher activation energy.

Our conclusion is that there is a chemically significant barrier between a linear geometry and both bent isomers, and that the *cis* isomer is discriminated against by steric problems — the R groups bumping into each other (which could be overcome by appropriate molecular design). The explanation of the substantial barrier between linear and *trans* isomer will be given in the next section.

The C_s geometry (and D_{2h}, too) seems like a small perturbation of the *trans* form. Close examination of the energetic and geometrical parameters in Table 1 shows the resemblance is very close — in energy, in M−M distance, and in the terminal M−R distance in the *trans* and C_s structures. Only the bridging M−R distances are longer in C_s geometries. Figure 6 shows for FMoMoF (one of the molecules for which the C_s is a global minimum, at least in our calculations) a transit from the C_s form to the *trans* C_{2h} one. The barrier is small. Examination of the results with other functionals and basis sets shows that the C_s minimum sometimes persists, sometimes not.

BrCrCrBr is the only case where a D_{2h} minimum is found. A transit $D_{2h} \rightarrow C_{2h} \rightarrow D_{\infty h}$ was studied (see Figure 4-SI in the Supporting Information); we found a small energy penalty for going to the *trans* form and from there the substantial barrier we had found before for reaching a linear geometry.

We conclude that the potential energy surface around the *trans* C_{2h} form is very soft. It costs very little energy to deform from C_{2h} to C_s. We do not trust our methods to say something decisively on the equilibrium geometry, except just what we said — the geometry is variable. Were any of these molecules to be realized in a crystal, packing energies would produce one or another geometry. Nature, it seems, is never simple — even in this short series of RMMR molecules.

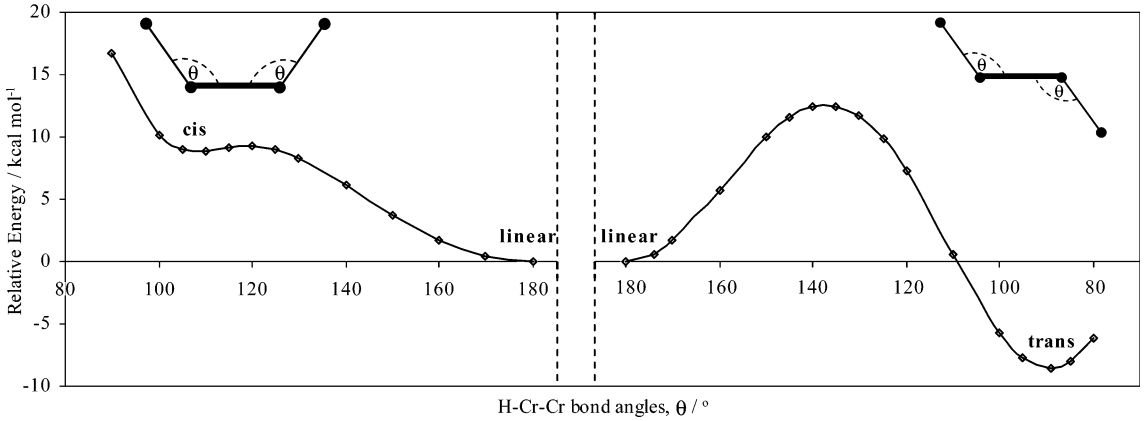

Figure 5. Optimized energies for symmetry constrained transits from (a) the *cis* to the linear and (b) the linear to the *trans* geometry of HCrCrH.

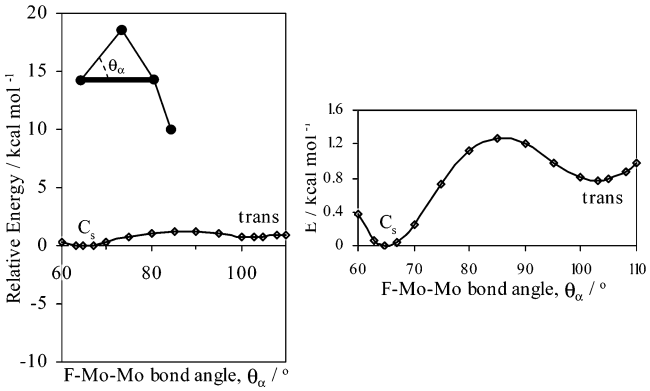

Figure 6. Optimized energies for symmetry-constrained transits from the C_s to the *trans* geometry of FMoMoF. For comparison, the energy and bond angle scales on the left are the same as for Figure 5; the picture on the right magnifies the energy scale.

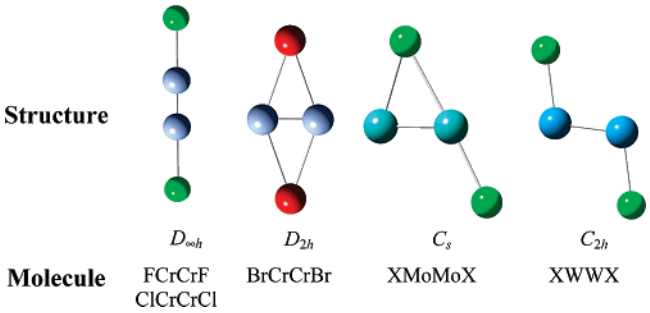

Figure 7. Pictorial summary of the global minima for XMMX molecules. Where X is not specified, that geometry is the minimum energy isomer for all three X = F, Cl, and Br. Geometrical parameters for all the optimized isomers are given in Table 1.

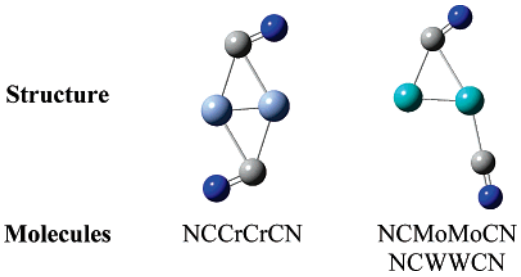

Figure 8. Representations of the minimum energy C_{2h} and C_s isomers of the NCMMCN molecules (M = Cr, Mo, and W). Geometric parameters for all the optimized isomers are given in Table 1.

Let us examine in greater detail the series of RMMR structures substituent by substituent (R = H, F, Cl, Br, CN, and Me).

HMMH. The *trans*-bent C_{2h} isomer (Figure 2, isomer 1) is the lowest energy isomer for all the hydrides. We will discuss this structural preference in the hydrides in the following sections, but we should point out that the computed stability of the C_{2h} structures is in agreement with earlier calculations by Landis and Weinhold,[28] who also found linear and *cis* minima.

XMMX. As mentioned previously, we obtained linear minimum energy structures for both FCrCrF and ClCrCrCl. The linear isomer for BrCrCrBr is very competitive, but the minimum energy doubly bridged D_{2h} structure is more stable by 3.4 kcal·mol^{-1}. A singly bridged XMoMoX molecule (C_s symmetry) is the lowest energy structure for X = F, Cl, and Br. Other isomers, such as the *trans*-bent C_{2h} and the linear $D_{\infty h}$ isomers, are nearby in energy (Table 1), but the C_s structure is always a bit more stable than they are. In the XWWX series, the *trans*-bent C_{2h} structure is the most stable isomer, with the linear and D_{2h} isomers being the least competitive geometries.

Reaching for a generality, we see that the structural preferences in the halide subset of the RMMR structures are essentially insensitive to the halide (see Figure 7) but show a strong dependence on the metal. This dependence of the relative energies of the isomers on M will be considered shortly.

NCMMCN. The cyano systems are necessarily more complex, as there are additional degrees of freedom in the position of the N and the M−C−N angle. In the chromium system, NCCrCrCN, the C_{2h} structure is the computed minimum energy geometry; in that structure (see Figure 8) the CCrCrC fragment is locally nearly D_{2h}. The C atoms are in an effectively bridging position between the two Cr atoms. The C−Cr bond that is adjacent to the C−N bond (215 pm) is a bit longer than the other C−Cr bond (210 pm). The possible involvement of the N atom in the bonding to the Cr_2 fragment is of interest for us, as well, because of the secondary interactions in ArCrCrAr. The N···Cr contact is 236 pm, which is really a bonding distance. In the NCMoMoCN and NCWWCN minimum energy C_s structures of Figure 8, the N···M contacts are 283 and 288 pm, respectively.

The preference for the C_s isomer (Figure 8) is unambiguous for the Mo and W cyano complexes. This isomer is close in energy to the C_{2h} structure, but that system is only a transition structure on the NCMoMoCN and NCWWCN potential energy surfaces (see Table 1-SI). The other isomers, including the linear one, are of noticeably higher energy and are uncompetitive.

MeMMMe. For the methyl-substituted system, we examined the range of geometries found for R = H, X. Of course, the situation is complicated by methyl group conformations, as is evident from Figures 3 and 1-SI. The linear, *trans*-bent, *cis*-bent, and other possible isomeric forms of the basic C−MM−C framework have a number of conformations of comparable energies, depending on how exactly the C−H bonds are oriented.

For the D_{3h} and D_{3d} linear variants, for instance, the energies of the isomers are very similar, differing by only ∼0.1 kcal mol^{-1} — suggesting an extremely low barrier to Me rotation in these molecules. Nonetheless, the D_{3d} (with methyls staggered) is a minimum, while the D_{3h} conformation is only a transition structure on the MeMMMe potential surfaces for M = Cr, Mo, and W.

In Table 1 and Figure 3, we have included the structural and energetic details for only the four isomers that are minima on the potential energy surface of at least one of the MeMMMe molecules. The data for the less competitive structures are given in the Supporting Information (Tables 1-S1 and 2-SI, and Figure 1-SI).

Our hope for MeMMMe was founded on what happens on going from Si_2H_2 to MeSiSiMe; namely, that the potential surface would be simplified, with only "classical" linear, *cis*-bent, and *trans*-bent minima remaining. This was not to happen, as Table 1 and Figure 3 show. Several independent geometrical minima remain. The important geometrical realizations follow the trends observed for R = H: the linear form is stabilized relative to the *trans*-bent global minimum as one goes from W to Mo to Cr (Table 1). The strange MeCrCrMe C_s structure is geometrically related to the unusual C_s structures we saw earlier and may be interpreted as a perturbed *trans* structure with a stabilizing interaction between the terminal methyl and both of the metal centers.

Dependence of the Structure Preferences on M

In the Cr series (Table 1), the doubly bridged D_{2h} structures become more stable relative to the C_{2h} isomer as X gets larger going from F to Cl and Br. This may be explained by an increase in the M−X distance in the M−X−M bridge as X gets larger (Table 1, the differential due to the size of the halogen), causing a decrease in the repulsion between the electrons in the M−M bond and the bridging X atoms. Notice, as well, a slight increase in the M−M−X bond angle (67° and 71° for the D_{2h} geometries of FCrCrF and BrCrCrBr, respectively, in Table 1), which reduces somewhat the ring strain in the bridge.

However, going from Cr to Mo and W, the doubly bridged D_{2h} structure is noticeably destabilized relative to the C_{2h} isomer, even for the chlorides and bromides. Here is a possible explanation for this destabilization: Notice that the M−M distances increase much more dramatically than do the M−Cl (or M−Br) distances going from M = Cr to M = Mo and W. The bridging R atom is therefore closer to the M−M bond in the Mo and W D_{2h} systems than it is in the Cr analogues. This increases repulsion between the bridging atom R and the M−M bond and destabilizes the bridge. We believe that this factor plays a role in explaining why the D_{2h} isomers of ClMMCl and BrMMBr are local minima for M = Cr but are typically second-order saddle points on the potential surfaces for M = Mo and W (see Table 1-SI). In the latter systems, the C_s or the C_{2h} isomer is preferred.

Bond Distances

In the hydrides, the M−M distances are longer and the M−H distances shorter in the *cis*- and *trans*-bent isomers than they are in the linear forms, suggesting optimal bonding in the nonlinear molecules, in agreement with Landis and Weinhold.[28]

This ordering is not observed in the halides in general; in some cases the M−X distances are longer in the *cis*- and *trans*-bent isomers. This may be explained by a repulsive interaction between the lone pairs on X and the electrons in the MM fragment as the X−M−M bond angle is decreased. It is also consistent with a general trend in transition metal complexes, where M−X bridging distances are longer than terminal ones.

For each of the RMMR molecules we have investigated, the linear isomer has the shortest MM bond compared to the other five isomers. We take this as a general indicator that bonding in these molecules is a compromise; the lowest energy structure is not the one that optimizes MM bonding (assuming the typical, but not universal, relationship between bond length and strength). At the other extreme, the C_{2v} *cis*-bent isomer typically has the longest MM bond. For the halides, the difference between the shortest and the longest MM bonds may be as much as 15 pm.

Interestingly, among the minimum energy structures (in bold in Table 1) the MM distances are rather insensitive to changes in R and the coordination environment, especially for Mo and W. For the lowest energy Mo and W structures, the change in the bond length as a function of R is never more than ∼5 pm.

For each of the substituents, R, the M−R bond lengths change significantly only in going from the nonbridging to the bridging complexes. The bond distances are some tens of picometers longer in the bridging compounds compared to the terminal M−R bonds.

A Closer Look at the Simple HMMH Case

It is time to try to understand some of the more striking differences between the isomers and their variation with R. The main features demanding explanation are the following:

(1) The existence of a substantial (10 kcal·mol^{-1} or more) barrier between the linear minima and the *trans* (and *cis*)-bent isomers. Could this be a forbidden reaction, with a level crossing? (2) The M−M distances in the *trans*- and *cis*-bent M_2H_2 isomers (**1** and **3**) are greater than that in the linear isomer (**2**) (see Table 1), and, conversely, the M−H distances in **1** and **3** are shorter than in **2**. This observation suggests an effective reduction in the occupation of the bonding orbitals of the MM fragment when it is not collinear with the H atoms.

In the classical picture,[3] a M−M quintuple bond has a $\sigma^2\pi^4\delta^4$ configuration. As mentioned earlier, much configurational mixing is at work in multiply bonded compounds of this kind. Recently, Brynda et al. showed that this is the major configuration in the *trans*-bent and the linear forms for PhCrCrPh (Ph = phenyl), with a total weight of 45% in the CASSCF wave function.[29] People have worried, of course, about the effect of ligand−metal interactions on the geometry of the Ar′CrCrAr′ complex. What we see in the present work (and this has also been found in extended Hückel (eH) calculations on the HMMH systems, which have no electron correlation at all) is that the energetic preference for some bending at the metal centers is there even for ligands as simple as H, and for a single configuration wave function.

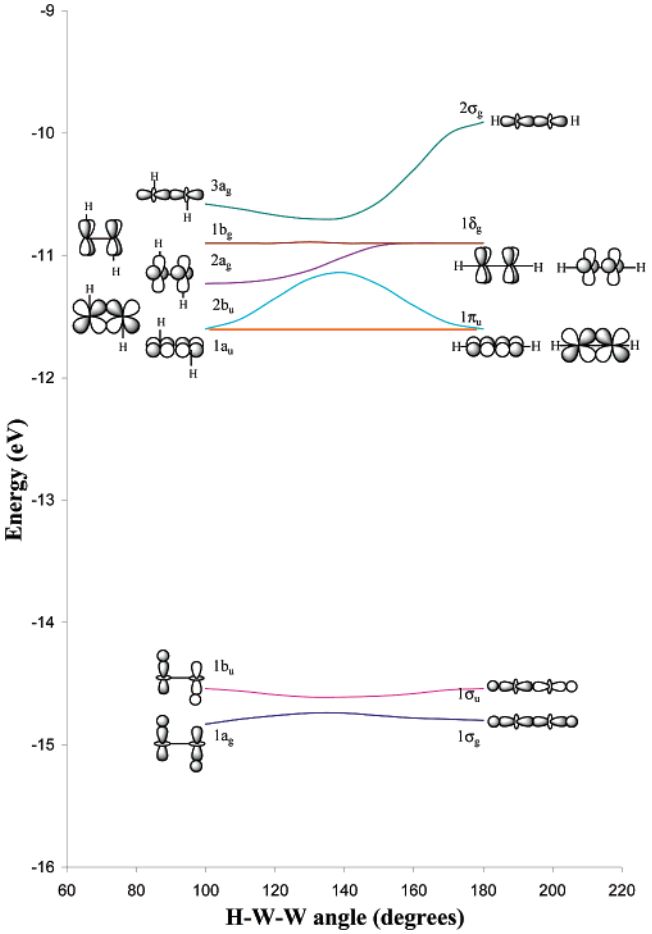

Figure 9. Walsh diagram for the highest occupied valence MOs of HWWH bending in *trans* fashion from the linear form to the linear form.

More generally we want to ask the question, what are the factors that make a given RMMR complex assume one structure over another?

To pursue this question we turn to the Walsh diagrams constructed using the eH method for HWWH (Figure 9). In this diagram the distances were kept fixed at the DFT optimized geometry of the linear form, varying only the HWW angle. The DFT-based Walsh diagrams were substantively similar.

Some key features of the diagram (Figure 9) are the following:

(1) The π, δ orbitals of the quintuple bond are easily identified in the linear form. However,

(2) the σ orbitals are somewhat more complicated, even in the linear geometry. There are two σ_g orbitals coming from the MM σ bond and the symmetric combination of the M−H bonds. Mixing of MM and MH σ bonding ensues; the orbital which is mainly MM σ is pushed up above the π and δ orbitals.

(3) One component of the π and δ orbitals, degenerate in the linear geometry, is unaffected by bending. In an all-electron calculation, its energy would change.

(4) The other component of the π and δ orbitals splits off. Starting from the linear geometry, one would expect these orbitals ($2b_u$, $2a_g$) to be destabilized, as ligand-field antibonding interactions between d orbitals and hydrogens are turned on. In fact, the $2a_g$ goes down in energy in Figure 9. This is a consequence of an avoided crossing with the rapidly sinking $3a_g$ orbital (which loses with bending its antibonding M−H interaction).[36]

(5) The $2b_u$ orbital goes through a maximum at $\theta = 135°$ — exactly where (antibonding) metal d and H interaction would be greatest. *That maximum is very important* — it is responsible for the existence of a substantial barrier between linear and bent minima in the HMMH systems.

The energy changes in the individual orbitals are pretty well understood; it is clear that the preference for the *trans* bending is set by the highest occupied molecular orbital (MO), $3a_g$, which is stabilized significantly in energy with bending.

Can the linear configuration ever be more stable than the *trans*-bent structure? Table 1 shows that this happens when hydrogen is substituted by a fluorine or a chlorine atom, which are π-donor ligands in RCrCrR. This effect, presumably due to better π overlap of the d_{xz} and d_{yz} orbitals with the 2p orbitals in the linear geometry, is not observed in the Mo and W analogues.

Table 2. Contribution (per Two Electrons) of Individual MOs to the Total Overlap Population between the Two W Atoms in the Linear and *Trans*-Bent HWWH Molecules

trans-bent		Linear	
MO	contribution to overlap population/*e*	MO	contribution to overlap population/*e*
$3a_g$	0.14	$2\sigma_g$	0.06
$1b_g$	0.12	$1\delta_g$	0.14
$2a_g$	0.41	$1\delta_g$	0.14
$2b_u$	0.32	$1\pi_u$	0.37
$1a_u$	0.35	$1\pi_u$	0.37
$1b_u$	0.00	$1\sigma_u$	−0.01
$1a_g$	0.03	$1\sigma_g$	0.04
total	1.37		1.11

Quintuple Bonding in All These Geometries?

The answer, briefly, is "yes, we think so." The chemical bond is a complex thing. On the experimental side, it is gauged by distances, force constants, energies, and spectroscopic and magnetic criteria. On the theoretical side, bonding is estimated by bond orders, overlap populations, and various topological properties of the electron density.

In theoretical calculations, one really has to try hard to estimate correlation and to distinguish significant bond formation from small antiferromagnetic coupling.[4] Our calculations are not of sufficient quality to judge this latter point. We retreat to a simpler procedure, of looking at the shape of the orbitals, computing various bond indices, and estimating overlap populations in a one-electron model. This may be simplistic, but it has been productive, both in producing understanding and in suggesting experiments.

First, Figure 9 for the HWWH molecule clearly shows five mainly d−d bonding orbitals filled. A similar picture is obtained for all the species studied. By the criterion of counting bonding orbitals, there are five bonds. But that is too simple. In this section we want to look at how much each filled MO contributes to the bonding, gauging the contribution by the Mulliken overlap population. Table 2 shows the individual MO contributions in the *trans*-bent and linear forms of HWWH. The lowest two orbitals are mostly WH bonding.

(36) In the case of HCrCrH and HMoMoH, see Supporting Information.

The overlap populations are interesting: π bonding contributes more than half of the overlap population in the linear molecule, and almost half in the *trans*-bent one. Though nonintuitive from the conventional wisdom in main group chemistry (where we have come to expect σ overlaps bigger than π overlaps), it is consistent with transition metal−metal overlaps — the WW $d_{xz}-d_{xz}$ overlap is the biggest one in the d block.

It is difficult to take apart σ and δ bonding in the *trans*-bent geometry as both a_g orbitals contain admixtures of W z^2 and x^2-y^2. The large contribution to the WW overlap population by the two electrons in $2a_g$ is striking; this orbital has important contributions to bonding from the W s and p orbitals in addition to W d.

Can we reason that RWWR has a quintuple bond from the absolute values of the WW overlap populations (1.37 and 1.11 for the linear and *trans*-bent, respectively)? Not directly. As a way into assessing the bonding between the MM centers, we did calculate overlap populations for H_nWWH_n units (with n = 2, 3, 4, 5) and observed a decrease in the overlap population as n got larger (and the WW bond weaker and longer).

In another approach to estimating the bonding, we obtained, using the density functional (BLYP) method, the metal−metal Wiberg indices for the optimized isomers of all the molecules calculated. The results are presented in Table 6-SI in the Supporting Information. The computed Wiberg bond indices all fall in the range 4.52−5.22, again supporting the existence of quintuple bonds across the wide range of RMMR geometries.

For all the molecules, the largest value for the MM Wiberg bond index is obtained for the linear isomers. This disagrees with the trend in Table 2 (there the *trans* structure has the greater Mulliken overlap population) but is completely consistent with our earlier observation that, of the RMMR isomers we considered, the linear isomers have the shortest MM bond. There appears to be a tradeoff between the MM and the MR bonding: the linear form has a stronger MM bond but a weaker M−R bond compared to other isomers with terminal R's. Importantly, the preferred nonlinear (*trans*, C_s, and D_{2h}) geometries (Table 1) are achieved without sacrificing the five-fold bonding character between the two metal centers (Table 4-SI).

Conclusions

We have explored in substantial detail the potential energy surfaces of RMMR molecules for M = Cr, Mo, W and for R = H, F, Cl, Br, CN, Me. A subsequent paper will approach the substituents of the experimentally observed systems with aryl substituents. We find a multitude of minima on the potential energy surface of these molecules. The most important ones are the linear and *cis*- and *trans*-bent ones. With two of the halogen substituents, linear geometries are the global minima in our calculations; for almost all the *trans*-bent or the C_s geometry is favored. The *cis*-bent minima are discouraged by a steric factor but with proper substituent engineering could become competitive. There is a particularly soft potential energy surface around the *trans*-bent minima, and in some of these molecules the real minima might be of C_s or even lower symmetry. The barrier between the bent and linear geometries is electronic in origin and readily traced to individual d orbitals. There is quintuple bonding, by simple criteria, in all of these geometries.

Acknowledgment. Financial support of G.M. was provided by AMC-ACS-Fomex. Our work was supported in Guanajuato by PROMEP-UGTO (Project UGTO-PTC-079). At Cornell, our work was supported by NSF grant CHE-0613306. Calculations were performed in part at the Cornell NanoScale Facility, a member of the National Nanotechnology Infrastructure Network, which is supported by the National Science Foundation (Grant ECS 03-35765). J.S.D. gratefully acknowledges that calculations performed at UW−Stevens Point were made possible through start-up funds provided by the College of Letters and Science and the Department of Chemistry.

Supporting Information Available: Appendix detailing computational methods employed and associated references; possible isomers of the MeMMMe molecules (M = Cr, Mo, and W); Walsh diagram for the highest occupied valence MOs of Cr_2H_2 obtained using BLYP/DZVP; optimized structures of the minimum energy $Cr_2(CN)_2$ C_{2h} structure, the high-energy D_{2h} $Mo_2(CN)_2$ structure, the high-energy $Mo_2(CN)_2$ $C_{2v}(1)$ structure, and the $Mo_2(CN)_2$ C_s structure; optimized energies for symmetry-constrained transits from the D_{2h} to the linear geometry of BrCrCrBr via a trans local maximum; number of imaginary frequencies obtained for the RMMR structures studied; selected geometric parameters and relative energies of six RMMR (R = H, F, Cl, Br, CN, and Me) isomers obtained at the BLYP and a series of alternative computational levels; M−M Wiberg indices obtained for the isomers found to be local minima on the potential energy surfaces of RMMR (R = H, F, Cl, Br, CN, and Me), at the BLYP level. This material is available free of charge via the Internet at http://pubs.acs.org.

JA075454B